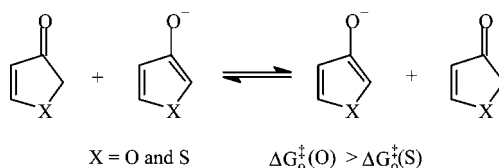# Deprotonation of 3(2H)-Furanone and 3(2H)-Thiophenone by Carbanions in the Gas Phase: Disproportionately High Aromaticity of the Transition State: An *Ab Initio* Study

Claude F. Bernasconi,*,[†] Hiroshi Yamataka,[‡] Nobuyoshi Yoshimura,[‡] and Makoto Sato[‡]

Department of Chemistry and Biochemistry, University of California, Santa Cruz, California 95064 and Department of Chemistry, Rikkyo University, Nishi-Ikebukuro 3-34-1, Toshima-ku, Tokyo, 171-8501, Japan

bernasconi@chemistry.ucsc.edu

Received August 12, 2008

X = O and S $\Delta G_o^{\ddagger}(O) > \Delta G_o^{\ddagger}(S)$

The reversible deprotonation of 3(2H)-furanone (**3H−O**) and 3(2H)-thiophenone (**3H−S**) by a series of delocalized carbanions and by CN⁻, and the identity proton transfer of **3H−O** to its conjugate base (**3⁻−O**) and of **3H−S** to **3⁻−S** have been studied at the MP2//6−31+G** level. The main objective has been to examine to what extent the aromaticity of **3⁻−O** and **3⁻−S** is expressed at the transition state of these reactions and how the intrinsic barriers are affected by the transition state aromaticity. Aromaticity parameters such as NICS values, HOMA and Bird Indices indicate a disproportionately high degree of aromatic stabilization of the transition state. This stabilization results in a reduction of the *intrinsic* barriers which is most clearly manifested in the identity reactions. However, these reductions are relatively modest compared to those reported previously for the identity proton transfers from the benzenium ion to benzene and of cyclopentadiene to its conjugate base, reflecting the smaller aromatic stabilization of **3⁻−O** and **3⁻−S** compared to those of benzene and cyclopentadienyl anion.

Introduction

We have recently become interested in reactions that generate aromatic products by deprotonation of nonaromatic precursors. Specifically we want to examine how much of the product aromaticity develops at the transition state and how it affects the intrinsic barrier[1] of these reactions. In a recent computational study of the carbon-to-carbon identity proton transfers of eqs 1 and 2[2] it was shown that there is a disproportionately large degree of aromaticity at the transition state of these reactions as indicated by their NICS[3] and HOMA[4] values. It was also shown that the intrinsic barriers of these reactions were substantially lower than the barriers of their corresponding noncyclic analogues, that is, eqs 3 and 4, respectively. Such a lowering of the intrinsic barriers
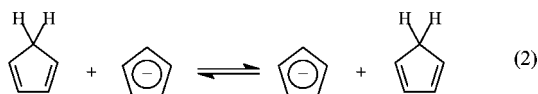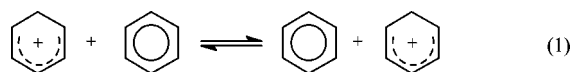
is consistent with the principle of nonperfect synchronization (PNS),[5] which states that a product stabilizing factor (aromaticity in our case) that develops ahead of bond changes reduces the intrinsic barrier of a reaction.[6]

† University of California.

‡ Rikkyo University.

(1) The intrinsic barrier refers to the barrier of a reaction for which there is no thermodynamic driving force ($\Delta G° = 0$); in solution phase reactions one often deals with intrinsic rate constants which are defined as $k_o = k_1 = k_{-1}$ when $K_1 = k_1/k_{-1} = 1$ where k_1 and k_{-1} refer to the rate constants in the forward and reverse directions, respectively.

(2) Bernasconi, C. F.; Wenzel, P. J.; Ragains, M. L. *J. Am. Chem. Soc.* **2008**, *130*, 4934.

(3) (a) Schleyer, P. v. R.; Maerker, C.; Dransfeld, A.; Jiao, H.; Hommes, N. J. R. v. E. *J. Am. Chem. Soc.* **1996**, *118*, 6317. (b) Chen, Z.; Wannere, C. S.; Corminboeuf, C.; Puchta, R.; Schleyer, P. v. R. *Chem. Rev* **2005**, *105*, 3842.

Similar conclusions were reached based on solution phase kinetic investigations of reactions such as eq 5 where B^ν are families of primary aliphatic amines and secondary alicyclic amines.[7]

1H-O (X = O)
1H-S (X = S)

1^-**-O** (X = O)
1^-**-S** (X = S)

(5)
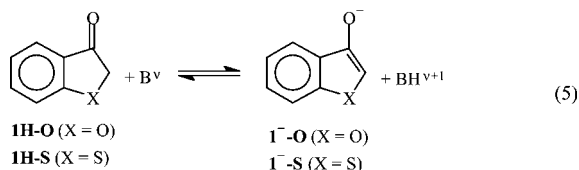
For example, for the reactions with secondary alicyclic amines the intrinsic rate constant $(k_o)^1$ for reaction 5 with X = S was found to be 10-fold higher (the intrinsic barrier $\Delta G_0^\ddagger$ to be 1.3 kcal/mol lower) than with X = O. Because 1^-−S is more aromatic than 1^-−O, the PNS implies that development of anion aromaticity at the transition state is ahead of proton transfer. Results along the same lines were also reported for reaction 6;[8] in this case, the order of the intrinsic rate constants was found

2H⁺-O (X = O)
2H⁺-Se (X = Se)
2H⁺-S (X = S)

2-O (X = O)
2-Se (X = Se)
2-S (X = S)

(6)
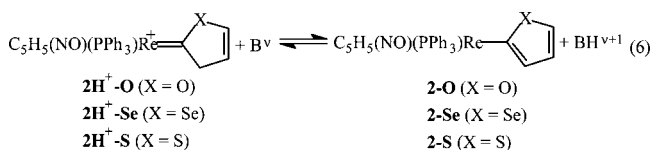
to be $k_o(\text{O}) < k_o(\text{Se}) < k_o(\text{S})$, again reflecting an increase with increasing aromaticity of the heterocycles furan < selenophene < thiophene.

The special interest in examining whether or not it may be generally true that the development of aromaticity has made more progress than proton transfer at the transition state derives from earlier findings according to which *resonance* and *charge delocalization* effects invariably *lag behind* proton transfer at the transition state,[5,9] thereby *increasing* the intrinsic barrier.[6] The reasons why, at the transition state, product aromaticity is much more strongly developed than product resonance/delocalization have been discussed elsewhere.[2]

Following up on the solution phase reactions of eq 5 we now report a computational study of the gas phase deprotonation of 3(2H)-furanone (**3H−O**) and 3(2H)-thiophenone (**3H−S**) by a series of carbanions, by CN⁻ and also of **3H−O** by 3^-−O and **3H−S** by 3^-−S.

3H-O (X = O)
3H-S (X = S)

3^-**-O** (X = O)
3^-**-S** (X = S)

(7)
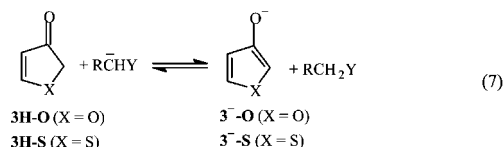
The calculated aromaticity indices show again a disproportionately high degree of aromaticity at the transition state for the reactions of both **3H−O** and **3H−S** which again results in a lowering of the respective intrinsic barriers. However, the

(4) Krygowski, T. M.; Cyránski, M. K. *Chem. Rev.* **2001**, *101*, 1385.
(5) (a) Bernasconi, C. F. *Acc. Chem. Res.* **1987**, *20*, 301. (b) Bernasconi, C. F. *Acc. Chem. Res.* **1992**, *25*, 9. (c) Bernasconi, C. F. *Adv. Phys. Org. Chem.* **1992**, *27*, 119.
(6) An important corollary to the PNS is that a product stabilizing factor that *lags behind* bond changes *enhances* the intrinsic barrier.
(7) Bernasconi, C. F.; Pérez-Lorénzo, M. *J. Am. Chem. Soc.* **2007**, *129*, 2704.
(8) Bernasconi, C. F.; Ragains, M. L.; Bhattacharya, S. *J. Am. Chem. Soc.* **2003**, *125*, 12328.
(9) For numerous citations of more recent work, see ref 2.

TABLE 1. Reaction Enthalpies ($\Delta H°$) and Activation Enthalpies ($\Delta H^\ddagger$) for the Reactions of Equation 7

RC̄HY	$\Delta H°$	$\Delta H^\ddagger$	BSSE[a]	$\Delta H_{corr}^\ddagger$ [b]
	kcal/mol	kcal/mol	kcal/mol	kcal/mol
	(3H-O) ($\Delta H_{acid}^o = 356.4$ kcal/mol)[c]			
1 ⁻CH₂CN	−19.8	−12.9	5.7	−7.2
2 ⁻CH₂CO₂H	−14.3	−8.2	6.0	−2.2
3 ⁻CH₂COCH₃	−13.0	−7.6	5.8	−1.8
4 ⁻CH₂CHO	−10.4	−7.2	5.9	−1.3
5 ⁻CH₂NO₂	−1.2	−4.7	5.7	1.1
6 CH₃C̄HNO₂	−0.9	−5.2	6.5	1.3
7 ⁻CH(CN)₂	19.8	1.2	6.3	7.5
	(3H-S) ($\Delta H_{acid}^o = 349.7$ kcal/mol)[c]			
1 ⁻CH₂CN	−26.5	−15.2	6.5	−8.7
2 ⁻CH₂CHO	−17.1	−10.9	6.7	−4.2
3 ⁻CH₂NO₂	−7.9	−8.8	7.2	−1.6
4 ⁻CH₂NO	−0.3	−3.5	6.4	2.9
5 ⁻CH₂CHS	1.3	−2.6	7.2	4.6
6 ⁻CH(CN)₂	13.1	−3.8	7.3	3.5
7 ⁻CH(NO₂)₂	24.7	4.1	9.1	13.2

[a] BSSE: Basis set superposition error. [b] $\Delta H_{corr}^\ddagger = \Delta H^\ddagger + $ BSSE. [c] ΔH_{acid} refers to the gas phase acidities of **3H−O** and **3H−S**, respectively.

reductions in the intrinsic barriers are much smaller than for reactions 1 and 2.

Results

All calculations were performed at the MP2/6−31+G** level. The computational details are reported in the Supporting Information.[10]

Reactions of 3H−O and 3H−S with Carbanions. The choice of carbanions was dictated by our goal to include bases of higher as well as of lower basicity than that of **3−O⁻** or **3−S⁻**. For the reaction of **3H−O** our set comprises, in order of decreasing basicity, ⁻CH₂CN, ⁻CH₂CO₂H, ⁻CH₂COCH₃, ⁻CH₂CHO, ⁻CH₂NO₂, CH₃C⁻HNO₂, and ⁻CH(CN)₂. For the reactions of **3H−S** which is 6.7 kcal/mol more acidic than **3H−O**, the following carbanions, again in order of decreasing basicity, were used: ⁻CH₂CN, ⁻CH₂CHO, ⁻CH₂NO₂, ⁻CH₂NO, ⁻CH₂CHS, ⁻CH(CN)₂, and ⁻CH(NO₂)₂.

Chart S1 of the Supporting Information[10] shows the transition state structures for the reactions of **3H−O** with the various carbanions whereas Chart S2[10] shows the transition states for the reactions of **3H−S**. The reaction enthalpies ($\Delta H°$) and reaction barriers ($\Delta H^\ddagger$) are summarized in Table 1 whereas Figures 1 and 2 show plots of $\Delta H^\ddagger$ versus $\Delta H°$. The barriers

(10) See paragraph concerning Supporting Information at the end of this paper.

FIGURE 1. Plot of $\Delta H^{\ddagger}_{corr}$ versus ΔH° for the reaction of **3H−O** with a series of carbanions; numbering refers to the numbers in Table 1.

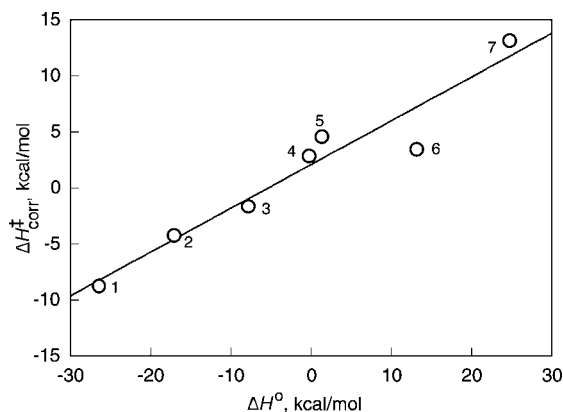**FIGURE 2.** Plot of $\Delta H^{\ddagger}_{corr}$ versus ΔH° for the reaction of **3H−S** with a series of carbanions; numbering refers to the numbers in Table 1.

include corrections for the basis set superposition errors (BSSE)[11] in the transition state energies.[12]

As a referee pointed out, many of the barriers ($\Delta H^{\ddagger}$) are negative. This is because, as in previous work,[13] we use the term barrier for the enthalpy difference between the transition state and the separated reactants and not between the transition state and the ion-dipole complexes which precede the transition state in gas phase ion−molecule reactions;[14] these ion−dipole complexes have little relevance with respect to the questions dealt with in the present work and hence have not been calculated.

Table 2 reports relevant transition state bond lengths, and absolute as well as percent changes in these bond lengths between the transition state and the reactants. Table 3 summarizes NICS values,[3] HOMA,[15] and Bird Indices[16] as measures of aromaticity of reactants, products, and transition states. Note that the various NICS values refer to different positions relative to the center of the aromatic ion as defined

CHART 1

by Chart 1. From the NICS values, the HOMA and Bird Indices we also calculated the % progress in the development of aromaticity at the transition state (Table 3); it is given by eq 8 where $I(TS)$, $I(R)$, and $I(P)$ represent the aromaticity index at the transition state, the reactant, and the product, respectively.

$$\%(TS) = 100\frac{I(TS) - I(R)}{I(P) - I(R)} \qquad (8)$$

Reactions of 3H−O, 3H−S, 4H−O, 4H−S, and other Carbon Acids with CN⁻. Data for a Brønsted plot of a different kind than those in Figures 1 and 2 were generated for the reactions of **3H−O, 3H−S, 4H−O, 4H−S**, and various other carbon acids with CN⁻. The results are summarized in Table 4 whereas Figure 3 shows the corresponding Brønsted plot.

Detailed Analysis of the Reactions of 3H−O with ⁻CH₂NO₂ and of 3H−S with ⁻CH₂NO. Further insight into how critical geometric parameters and aromaticity develop along the reaction coordinate was sought by subjecting the reaction of **3H−O** with $^{-}CH_2NO_2$ and the reaction of **3H−S** with $^{-}CH_2NO$ to calculations of r_{C-H} and r_{H-B} as well as the NICS parameters and the Bird Index. Figures 4 and S1 (see Supporting Information)[10] show plots of r_{C-H} and r_{H-B} as a function of the reaction coordinate (IRC) for **3H−O** and **3H−S**, respectively; Figures 5 and S2 (see Supporting Information)[10] show plots of the NICS parameters versus r_{C-H} for **3H−O** and **3H−S**, respectively; Figures 6 and S3 (see Supporting Information)[10] show plots of the Bird Index versus r_{C-H} for **3H−O** and **3H−S**, respectively.

Identity Proton Transfers Between 3H−X and 3⁻−X. Equation 9 represents identity proton transfers similar to eqs 1 and 2. The aromaticity indices for the transition states are summarized in Table 5 whereas the barriers are reported in Table 6; included in Table 6 are the barriers of the noncyclic reference identity reactions of eq 10.

3H-O (X = O)   **3⁻-O** (X = O)   **3⁻-O** (X = O)   **3H-O** (X = O)
3H-S (X = S)   **3⁻-S** (X = S)   **3⁻-S** (X = S)   **3H-S** (X = S)

$CH_2{=}CH{-}\overset{O}{\overset{\|}{C}}{-}CH_2XCH_3$ + $CH_2{=}CH{-}\overset{O^-}{\overset{\|}{C}}{=}CHXCH_3$

4H-O (X = O)   **4⁻-O** (X = O)
4H-S (X = S)   **4⁻-S** (X = S)

$$(10)$$

$\Longrightarrow$ $CH_2{=}CH{-}\overset{O^-}{\overset{\|}{C}}{=}CHXCH_3$ + $CH_2{=}CH{-}\overset{O}{\overset{\|}{C}}{-}CH_2XCH_3$

4⁻-O (X = O)   **4H-O** (X = O)
4⁻-S (X = S)   **4H-S** (X = S)

(11) Boys, S. F.; Bernardi, F. *Mol. Phys.* **1970**, *19*, 553.

(12) The BSSE corrections reported are those calculated for the three fragment system proton + two anionic fragments, by using the counterpoise keyword in Gaussian03. For the reactions of furanone and thiophenone with a series bases, BSSE corrections were also calculated for two fragment systems (in two ways, Ar⁻ + H−Base and Ar−H + Base⁻). The sizes of the corrections for two fragments gave linear correlation vs. those for three fragments with slope of 1.00 ± 0.05 with $R_2 = 0.999$.

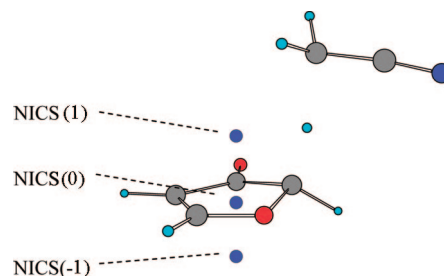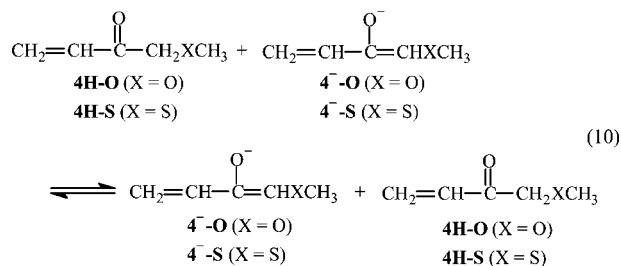(13) Reference 2 and numerous references cited therein.

(14) (a) Farneth, W. E.; Brauman, J. I. *J. Am. Chem. Soc.* **1976**, *98*, 7891. (b) Moylan, C. R.; Brauman, J. I. *Annu. Rev. Phys. Chem.* **1983**, *34*, 187.

(15) Krygowski, T. M.; Cyránski, M. K. *Chem. Rev.* **2001**, *101*, 1385.

(16) (a) Bird, C. W. *Tetrahedron* **1985**, *41*, 1409. (b) Bird, C. W. *Tetrahedron* **1986**, *42*, 89. (c) Bird, C. W. *Tetrahedron* **1992**, *48*, 335.

TABLE 2. Relevant Transition State Bond Lengths for the Reactions of Equations 7 and 9

| B[−a]	$\Delta H°$ kcal/mol	r_{C-H} Å	r_{H-B} Å	$r_{C=C}$ Å	$\Delta r_{C=C}$[b] Å (%)	r_{C-CO} Å	Δr_{C-CO}[c] Å (%)	$r_{C=O}$ Å	$\Delta r_{C=O}$[d] Å (%)
				3H−O					
−CH₂CN	−19.8	1.233	1.665	1.361	0.006 (43)	1.464	−0.067 (54)	1.251	0.020 (31)
−CH₂COOH	−14.3	1.297	1.531	1.362	0.007 (52)	1.464	−0.067 (54)	1.257	0.026 (41)
−CH₂COOH₃	−13.0	1.305	1.518	1.362	0.007 (50)	1.465	−0.066 (53)	1.258	0.027 (42)
−CH₂CHO	−10.4	1.301	1.518	1.363	0.008 (57)	1.463	−0.068 (55)	1.258	0.027 (42)
−CH₂NO₂	−1.2	1.327	1.467	1.362	0.007 (50)	1.464	−0.067 (54)	1.257	0.026 (41)
CH₃C̄HNO₂	−0.9	1.328	1.445	1.363	0.008 (57)	1.463	−0.068 (55)	1.258	0.027 (42)
3⁻−O	*0.0*	*1.391*	*1.391*	*1.363*	*0.008 (57)*	*1.425*	*−0.106 (35)*	*1.261*	*0.030 (47)*
−CH(CN)₂	19.8	1.438	1.362	1.362	0.007 (50)	1.447	−0.084 (68)	1.262	0.033 (52)
				3H−S					
−CH₂CN	−26.5	1.191	1.783	1.361	0.006 (30)	1.489	−0.048 (41)	1.248	0.016 (27)
−CH₂CHO	−17.1	1.283	1.548	1.363	0.008 (40)	1.470	−0.067 (57)	1.256	0.024 (40)
−CH₂NO₂	−7.9	1.296	1.495	1.364	0.009 (45)	1.471	−0.066 (56)	1.257	0.025 (42)
−CH₂NO	−0.3	1.404	1.356	1.366	0.011 (55)	1.458	−0.079 (67)	1.263	0.031 (52)
3⁻−S	*0.0*	*1.382*	*1.382*	*1.366*	*0.011 (55)*	*1.459*	*−0.078 (66)*	*1.263*	*0.031 (52)*
−CH₂CHS	1.3	1.408	1.354	1.365	0.010 (50)	1.457	−0.080 (68)	1.263	0.031 (52)
−CH(CN)₂	13.1	1.382	1.411	1.364	0.009 (45)	1.459	−0.078 (66)	1.261	0.029 (43)
−CH(NO₂)₂	24.7	1.452	1.317	1.364	0.009 (45)	1.457	−0.080 (68)	1.262	0.030 (50)

[a] B = RC̄HY. [b] $\Delta r_{C=C} = r_{C=C}(TS) - r_{C=C}(3H-X)$ with $r_{C=C}(3H-O) = 1.355$ Å, $r_{C=C}(3^-−O) = 1.369$ Å, $r_{C=C}(3H-S) = 1.355$ Å, $r_{C=C}(3^-−S) = 1.375$ Å. [c] $\Delta r_{C-CO} = r_{C-CO}(TS) - r_{C-CO}(3H-X)$ with $r_{C-CO}(3H-O) = 1.531$ Å, $r_{C-CO}(3^-−O) = 1.407$ Å, $r_{C-CO}(3H-S) = 1.537$ Å, $r_{C-CO}(3^-−S) = 1.419$ Å. [d] $\Delta r_{C=O} = r_{C=O}(TS) - r_{C=O}(3H-X)$ with $r_{C=O}(3H-O) = 1.231$ Å, $r_{C=O}(3^-−O) = 1.295$ Å, $r_{C=O}(3H-S) = 1.232$ Å, $r_{C=O}(3^-−O) = 1.292$ Å.

TABLE 3. Transition State Aromaticity Indices for the Reactions of Equation 7

RCHY	$\Delta H°$ kcal/mol	NICS(0)	NICS(1)	NICS(−1)	HOMA	Bird Index	NICS(0)	NICS(1)	NICS(−1)	HOMA	Bird Index
								percent progress at TS			
						3H−O[a]					
−CH₂CN	−19.8	−3.36	−4.68	−3.89	−0.097	28.99	25.0	51.6	33.3	47.9	35.9
−CH₂CO₂H	−14.3	−5.28	−5.04	−4.70	0.083	32.58	45.4	60.1	52.1	62.6	56.3
−CH₂COCH₃	−13.0	−5.49	−5.44	−4.64	0.105	32.81	47.6	69.4	50.7	64.4	57.6
−CH₂CHO	−10.4	−6.59	−6.73	−4.99	0.132	34.04	59.3	99.5	59.0	66.6	64.6
−CH₂NO₂	−1.2	−5.36	−5.04	−4.92	0.115	33.34	46.3	60.0	57.3	65.2	60.6
CH₃C̄HNO₂	−0.9	−5.15	−4.86	−4.76	0.126	34.04	44.0	55.9	53.5	66.1	64.6
−CH(CN)₂	19.8	−5.98	−5.10	−5.04	0.245	33.89	52.8	61.4	60.2	75.8	63.7
						3H−S[b]					
−CH₂CN	−26.5	−4.33	−4.15	−3.71	−0.188	42.46	24.7	34.1	25.9	46.3	33.9
−CH₂CHO	−17.1	−6.21	−5.39	−4.69	0.062	48.19	45.3	59.6	46.0	64.5	51.3
−CH₂NO₂	−7.9	−5.88	−4.84	−4.92	0.082	48.91	41.6	48.4	50.7	65.9	53.5
−CH₂NO	−0.3	−7.46	−6.04	−5.43	0.248	54.17	58.9	73.1	61.0	77.6	69.5
−CH₂CHS	1.3	−7.75	−6.49	−5.55	0.196	53.79	62.1	82.2	63.6	71.2	68.3
−CH(CN)₂	13.1	−6.36	−4.95	−5.03	0.136	51.31	46.9	50.6	52.9	73.9	60.8
−CH(NO₂)₂	24.7	−6.59	−5.52	−5.42	0.236	53.08	49.4	62.4	60.8	76.7	66.2

[a] **3H−O/3⁻−O**: NICS(0) −1.00/−10.48, NICS(1) − 2.48/−6.74, NICS(−1) −2.47/−6.74, HOMA −0.686/0.544, Bird Index 22.68/40.28. [b] **3H−S/3⁻−S**: NICS(0) −2.07/−11.21, NICS(1) −2.49/−7.35, NICS(−1) −2.45/−7.33, HOMA −0.854/0.566, Bird Index 31.31/64.20.

Aromatic Stabilization Energies (ASE). An attempt to estimate aromatic stabilization energies was based on the $\Delta H°$ values of the isodesmic reactions of eq 11. For reasons explained in the Discussion, the values obtained from these reactions are probably not very reliable.

$$^2H° = -13.40 \text{ kcal/mol} \quad (11a)$$

$$^2H° = -14.83 \text{ kcal/mol} \quad (11b)$$
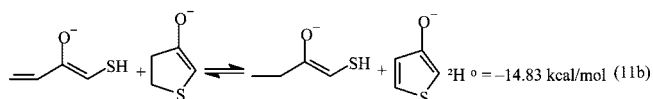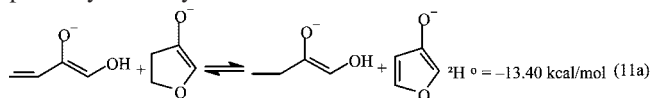
Discussion

Reactions of 3H−O and 3H−S with Carbanions. A. Energies and Geometries. The plots of $\Delta H^{\ddagger}$ versus $\Delta H°$

shown in Figures 1 and 2 are equivalent to enthalpic Brønsted plots. Despite some scatter, these plots are remarkably linear. The scatter in both plots may be mainly attributed to differences in the intrinsic barriers to the protonation of the various carbanions that arise from differences in the inductive, resonance, and polarizability effects of the Y-group of RC̄HY as well as differences in steric crowding of the transition state.[5,17] In fact, in view of these differences in the intrinsic barriers which may be quite substantial[5,17] it is perhaps surprising that the scatter in Figures 1 and 2 is not more pronounced.[18]

The slopes of these plots, β, are 0.33 ± 0.04 for **3H−O** and 0.39 ± 0.05 for **3H−S**, respectively. Within the framework of

(17) Bernasconi, C. F.; Pérez-Lorénzo, M.; Brown, S. D. *J. Org. Chem.* **2007**, *72*, 4416.
(18) The fact that in the gas phase the effect of resonance on intrinsic barriers is less pronounced than in solution[19] may be partly responsible for the weak scatter.
(19) Bernasconi, C. F.; Wenzel, P. J. *J. Org. Chem.* **2001**, *66*, 968.

TABLE 4. Reactions of 3H−O, 3H−S, 4H−O, 4H−S, and Various Other Carbon Acids with CN−

	carbon acid	$\Delta H°$ kcal/mol	$\Delta H^\ddagger$ kcal/mol	$BSSE^a$ kcal/mol	$\Delta H_{corr}^{\ddagger}{}^b$ kcal/mol
1	$CH_2(NO_2)_2$	−24.7	−24.1	4.4	−19.7
2	$CH_2(CN)_2$	−13.0	−22.3	4.3	−18.0
3	$CH_2(CHO)_2$	−12.6	−13.3	3.9	−9.4
4	$CH_3COCH_2COCH_3$	−10.2	−14.2	4.3	−9.9
	3H−S	0.0	−8.2	5.0	−3.2
	4H−S	0.1	−7.4	4.8	−2.6
5	$CH_3COCHCl_2$	1.8	−15.1	6.3	−8.8
	3H−O	6.7	−4.0	4.1	0.1
6	$CH_3CH_2NO_2$	7.6	−5.9	4.1	−1.8
	4H−O	7.7	−1.2	4.3	3.1
7	CH_3NO_2	7.9	−5.5	3.6	−1.9
8	CH_3COCH_3	19.7	3.7	3.7	7.4
9	CH_3CONH_2	27.4	8.5	3.7	12.3

^{a} BSSE = Basis set superposition error. ^{b} $\Delta H_{corr}^{\ddagger} = \Delta H^\ddagger + BSSE$.
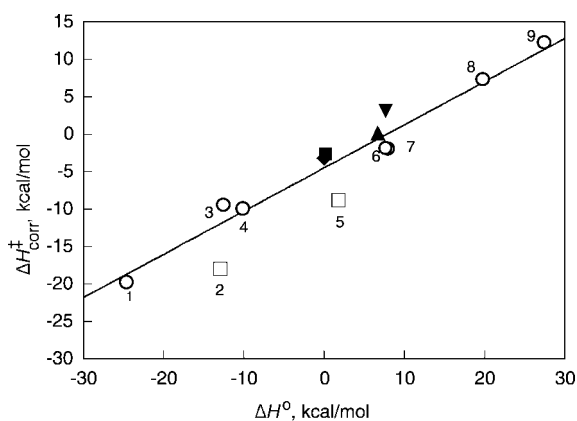

FIGURE 3. ○: Plot of $\Delta H_{corr}^{\ddagger}$ versus $\Delta H°$ for the reaction of a series of carbon acids with CN−; numbering refers to the numbers in Table 6. ◆: Reaction of **3H−S** with CN−. ■: Reaction of **4H−S** with CN−. ▲: Reaction of **3H−O** with CN−. ▼: Reactions of **4H−O** with CN−.

TABLE 5. Aromaticity Indices for the Identity Proton Transfers of Equation 9

species	NICS(0)	NICS(1)	NICS(−1)	HOMA	Bird Index
3H−O	−1.00	−2.48	−2.47	−0.686	22.68
TS	−7.12	−7.08	−5.46	0.217	36.76
3−−O	−10.43	−6.74	−6.74	0.544	40.28
% progress at TS	64.9	107.9	69.9	73.4	80.0
3H−S	−2.07	−2.49	−2.45	−0.854	31.31
TS	−6.66	−5.16	−5.37	0.231	53.19
3−−S	−11.21	−7.35	−7.33	0.566	64.20
% progress at TS	50.2	55.0	59.8	76.4	66.5

the Hammond[20]−Leffler[21] postulate, these β values suggest transition states that are somewhat more reactant-like than product-like. However, such an interpretation is an oversimplification; this can be seen from other probes of transition state structure which indicate that transition state structure changes significantly as a function of $\Delta H°$. The most dramatic manifestation of these changes is seen in the position of the proton-in-flight, as reflected in the r_{C-H} and r_{H-B} values (Table 2). For **3H−O**, r_{C-H} increases from 1.233 Å for the most favorable reaction (B− = −CH_2CN, $\Delta H° = -19.8$ kcal/mol) to 1.438 Å for the least favorable reaction (B− = −CH(CN)_2, $\Delta H° = 19.8$ kcal/mol), while r_{H-B} decreases from 1.665 Å for B− =

−CH_2CN to 1.362 Å for the B− = −CH(CN)_2. For **3H−S**, r_{C-H} increases from 1.191 Å for the most favorable reaction (B− = −CH_2CN, $\Delta H° = -26.5$ kcal/mol) to 1.452 Å for the least favorable reaction (B− = −CH(NO_2)_2, $\Delta H° = 24.7$ kcal/mol), while r_{H-B} decreases from 1.783 Å for the reaction with −CH_2CN to 1.317 Å for the reaction with −CH(NO_2)_2. These changes indicate movement toward more product-like transition states as the reaction becomes less favorable, as expected based on the Hammond[20]−Leffler[21] postulate. None of the reactions, except for the identity reactions of eq 9, have a completely symmetrical transition state with $r_{C-H} = r_{H-B}$ but the trend in the r_{C-H} and r_{H-B} values suggests that for both **3H−O** and **3H−S** this point is close to $\Delta H° = 0$; more specifically, for **3H−O**, this point is expected to occur at a slightly positive $\Delta H°$ value, for **3H−S** at a slightly negative $\Delta H°$ value.

In contrast to r_{C-H} and r_{H-B}, other geometric parameters such as $r_{C=C}$, r_{C-CO}, and $r_{C=O}$ change only slightly as a function of $\Delta H°$ (Table 2). Nevertheless, the changes are again in the direction of a more product-like transition state as the reaction becomes less favorable.

The intercepts of the Brønsted plots ($\Delta H^\ddagger$ for $\Delta H° = 0$) may be regarded as approximate values of the enthalpic intrinsic barrier ($\Delta H_0^\ddagger$); for **3H−O**, $\Delta H_0^\ddagger = 1.50 \pm 0.51$ kcal/mol, for **3H−S** $\Delta H_0^\ddagger = 2.09 \pm 0.79$ kcal/mol. The fact that these $\Delta H_0^\ddagger$ values are about the same within the rather large error limits is open to various interpretations. One is that the aromaticity of 3^--O and 3^--S simply does not affect the intrinsic barriers in a noticeable way. In view of the results for reactions 1, 2, 5, and 6, this is an unattractive interpretation. Another is that aromaticity does influence the intrinsic barriers but the difference in the aromaticity between 3^--O and 3^--S is too small to lead to a significant difference in the $\Delta H_0^\ddagger$ values. Assuming that the $\Delta H°$ values for eqs 11a and 11b are a true measure of the ASEs, their small difference may support such an interpretation. However, as discussed later, the difference in the $\Delta H°$ values for eqs 11a and 11b are probably not a true reflection of the differences in the ASEs and thus this interpretation is unconvincing. A third interpretation is that, because the sets of bases used in the two Brønsted plots are quite different,[22] this may affect the intrinsic barriers sufficiently as to mask the effect of the differences in the aromaticity of 3^--O and 3^--S.

A more reliable and more sensitive probe of the effect of aromaticity on the intrinsic barriers is to examine the $\Delta H_0^\ddagger$ values for the identity reactions of eq 9 (Table 6). It is more reliable because it avoids the problems of using different sets of bases in the Brønsted plots of Figures 1 and 2; it is more sensitive because the potential barrier-lowering PNS effect is doubled since there is both early development of product aromaticity as well as late loss of reactant aromaticity.[23] Indeed, $\Delta H_{0,corr}^\ddagger$ for the **3H−S/3−−S** system (2.3 kcal/mol) is 1.3 kcal/mol lower than for the **3H−O/3−−O** system (3.6 kcal/mol) which is reminiscent of the results for the solution phase reaction 5 and consistent with the notion that the greater aromaticity of 3^--S should lead to a lower barrier. The same qualitative conclusion is reached by comparing the **3H−X/3−−X** systems with their corresponding noncyclic reference systems **4H−X/4−−X** (eq 10): $\Delta H_{0,corr}^\ddagger$ for the **3H−O/3−−O** system is 1.8 kcal/mol lower
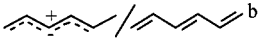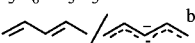
(20) Hammond, G. S. *J. Am. Chem. Soc.* **1955**, 77, 334.
(21) Leffler, J. E.; Grunwald, E. *Rates and Equilibria of Organic Reactions*; Wiley & Sons: New York, 1963.

(22) There are only three bases that are common to both Brønsted plots: −CH_2CN, −CH_2NO_2, and −CH(CN)_2.
(23) An additional corollary to the PNS5 is that a *reactant* stabilizing factor whose loss lags behind bond changes also lowers the intrinsic barrier while a reactant stabilizing factor whose loss is ahead of bond changes increases the intrinsic barrier.

TABLE 6. Barriers for the Identity Proton Transfers of Equations 9 and 10 and for the Previously Reported Reactions of Equations 1−4

Systems	Eq	$\Delta H^{\ddagger}$	$BSSE^c$	$\Delta H^{\ddagger}_{0,corr}$ [d]	$\Delta\Delta H^{\ddagger}_{0,corr}$ [e]
		kcal/mol	kcal/mol	kcal/mol	kcal/mol
3H-O/3⁻-O[a]	9	−3.5	7.1	3.6	−1.8
4H-O/4⁻-O[a]	10	−2.3	7.7	5.4	
3H-S/3⁻-S[a]	9	−7.0	9.3	2.3	−2.0
4H-S/4⁻-S[a]	10	−4.4	8.7	4.3	
$C_6H_7^+/C_6H_6$[b]	1	−12.7	5.1	−7.6	−11.1
⌇⌇⌇⁺⌇⌇ / ⌇⌇⌇⌇[b]	3	1.0	2.5	3.5	
$C_5H_6/C_5H_5^-$[b]	2	−2.7	4.9	2.2	−7.6
⌇⌇⌇⌇ / ⌇⌇⌇⌇[b]	4	6.4	3.4	9.8	

[a] This work (MP2//6-31+G(d,p)). [b] Reference 2 (MP2//6-311+G(d,p)). [c] BSSE = Basis set superposition error. [d] $\Delta H^{\ddagger}_{0,corr} = \Delta H^{\ddagger}_0 + BSSE$. [e] $\Delta\Delta H^{\ddagger}_{0,corr} = \Delta H^{\ddagger}_{0,corr,cyclic} - \Delta H^{\ddagger}_{0,corr,linear}$.
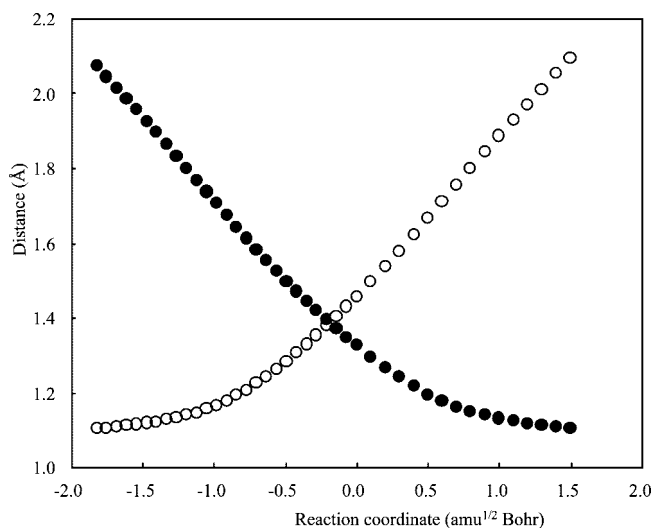

FIGURE 4. Plots of r_{C-H} (○) and r_{H-B} (●) versus IRC for the reaction of **3H−O** with $^-CH_2NO_2$.

than for the **4H−O/4⁻−O** system while $\Delta H^{\ddagger}_{0,corr}$ for the **3H−S/3⁻−S** system is 2.0 kcal/mol lower than for the **4H−S/4⁻−S** system, i.e. in both cases the aromatic system has a lower intrinsic barrier than the respective noncyclic reference system.

B. Aromaticity Indices. To gain further insights into the question as to whether aromaticity really develops ahead of proton transfer, we calculated the transition state aromaticity indices for reactions 7 (Table 3) as well as for the identity reactions of eq 9 (Table 5). Among the three NICS values (see Table 3), NICS(−1) is probably the most reliable[24] and we shall focus the discussion mainly on these values. The trends in the NICS values, the HOMA and Bird Indices for reaction 7 show a clear increase as the transition states become more product-

(24) As a general proposition, NICS values 1 Å above (NICS(1)) or below (NICS(−1)) the plane of the aromatic ring are regarded as being a better measure of the π-electron delocalization than NICS (or NICS(0)) which refer to the position at the center of the aromatic ring.[25] In our system, the position below the aromatic ring (NICS(−1)) seems to be the best choice because it avoids interference with the other components of the transition state.

(25) (a) Schleyer, P. v. R.; Jiao, H.; Hommes, N. J. R. v. E.; Malkin, V. G.; Malkina, O. *J. Am. Chem. Soc.* **1997**, *119*, 12669. (b) Schleyer, P. v. R.; Manoharan, M.; Wang, Z. X.; Kiran, B.; Jiao, H.; Puchta, R.; Hommes, N. J. R. v. E. *Org. Lett* **2001**, *3*, 2465.
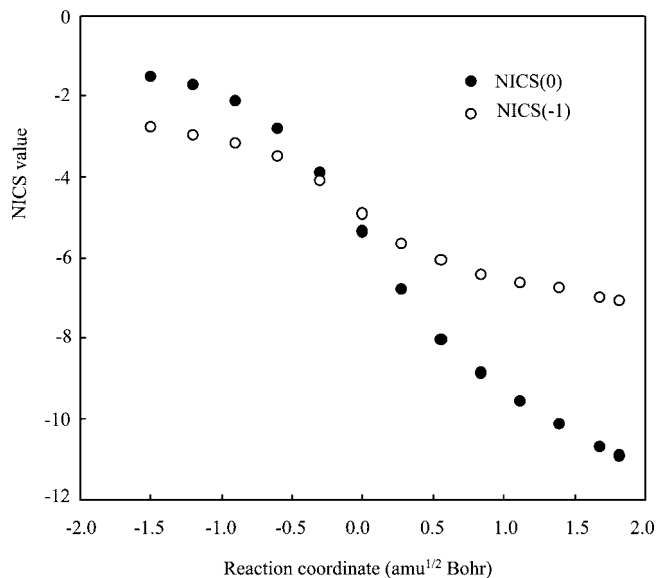
like with increasing $\Delta H°$, indicating an increase in aromaticity. Even more revealing is the % progress at the transition state calculated from eq 8. These % progress values indicate that this progress is not only >50% for the endothermic reactions (product-like transition states) but even for most of the exothermic reactions (reactant-like transition states) except those with very negative $\Delta H°$ values. This suggests that development of aromaticity is more advanced than proton transfer.

Another approach was to analyze changes in the r_{C-H} and r_{H-B} values and the aromaticity parameters as a function of reaction progress for the reactions of **3H−O** with $^-CH_2NO_2$ and the reaction of **3H−S** with $^-CH_2NO$, respectively. These reactions were chosen because they are nearly thermoneutral, with $\Delta H° = -1.2$ kcal/mol for the former and $\Delta H° = -0.3$ kcal/mol for the latter reaction and have fairly symmetrical transition states with r_{C-H} and r_{H-B} being quite similar to each other (Table 2).

Figures 4 and S1 (see Supporting Information)[10] show plots of r_{C-H} and r_{H-B} as a function of IRC for the reactions of **3H−O** with $^-CH_2NO_2$ and of **3H−S** with $^-CH_2NO$, respectively. For the reaction of **3H−O** we note that the point where $r_{C-H} = r_{H-B}$ occurs at a slightly positive IRC value while for the reaction of **3H−S** it occurs at a slightly negative value. These findings are consistent with the trends in the transition state r_{C-H} and r_{H-B} values reported in Table 2 discussed earlier. Specifically, for the reactions of **3H−O** with $R\bar{C}HY$ a transition state where $r_{C-H} = r_{H-B}$ is expected for the reaction with a hypothetical $R\bar{C}HY$ for which $\Delta H°$ is slightly positive while for the reaction of **3H−S** a transition state where $r_{C-H} = r_{H-B}$ is expected for the reaction with a $R\bar{C}HY$ for which $\Delta H°$ is slightly negative.

Figures 5 and S2 (see Supporting Information)[10] show plots of the NICS parameters versus the IRC for the reactions of **3H−O** with $^-CH_2NO_2$ and of **3H−S** with $^-CH_2NO$, respectively, whereas Figures 6 and S3 (see Supporting Information)[10] show the corresponding plots of the Bird Index versus the IRC.

The plots in Figures 5, S2 (see Supporting Information), 6, and S3 (see Supporting Information)[10] show a rather steep rise in the aromaticity of the reaction system as function of the IRC as the transition state is approached and a pronounced leveling off toward the value of the anionic product once the transition

FIGURE 5. Plots of NICS(0) and NICS(-1) versus IRC for the reaction of **3H−O** with $^-CH_2NO_2$.

FIGURE 6. Plots of the Bird Index versus IRC for the reaction of **3H−O** with $^-CH_2NO_2$.

state has been traversed. As indicated in Table 3, the % progress in the development of product aromaticity at the transition state of the reaction of **3H−O** with $^-CH_2NO_2$ is 57.3 for NICS(-1) and 60.6 for the Bird Index, while for the reaction of **3H−S** with $^-CH_2NO$ these percentages are 61.0 and 69.5, respectively. The somewhat lower percentages for the reaction of **3H−O** with $^-CH_2NO_2$ are consistent with a slightly earlier transition state (r_{C-H} = 1.327 Å, r_{H-B} = 1.457 Å) compared to the reaction of **3H−S** with $^-CH_2NO$ (r_{C-H} = 1.406 Å, r_{H-B} = 1.356 Å). Our analysis clearly shows that aromaticity is highly developed at the transition state.

The same conclusions are reached by examining the aromaticity indices for the identity reactions. In these reactions proton transfer is exactly half-complete at the transition state and hence the % progress of the aromaticity indexes which is >50% in all cases again indicates a disproportionately large degree of transition state aromaticity.

NICS values have been found to overestimate transition state aromaticity of certain thermally allowed reactions such as cycloadditions.[26] As suggested by a referee, this could possibly be the case in our systems as well, even though the reactions studied are proton transfers. However, the fact that the percent progress in aromaticity development calculated based on the NICS(-1) values are actually somewhat lower than those calculated from the HOMA and Bird Indices argues against an overestimate based on NICS(-1). The same is true for reactions 1 and 2 reported earlier.[2]

Reactions of 3H−O, 3H−S, and Other Carbon Acids with CN$^-$. The results are summarized in Table 4, and Figure 3 shows a Brønsted type plot of $\Delta H^\ddagger$ versus $\Delta H°$. The scatter in the plot may again be attributed to differences in the intrinsic barriers for the deprotonation of the various carbon acids that arise from differences in the interaction mechanisms responsible for the stabilization of the corresponding carbanions. The most pronounced deviations from the least-squares line are the points for $CH_2(CN)_2$ and $CH_3COCHCl_2$ (identified by squares in Figure 3). Both show strong negative deviations which are likely due

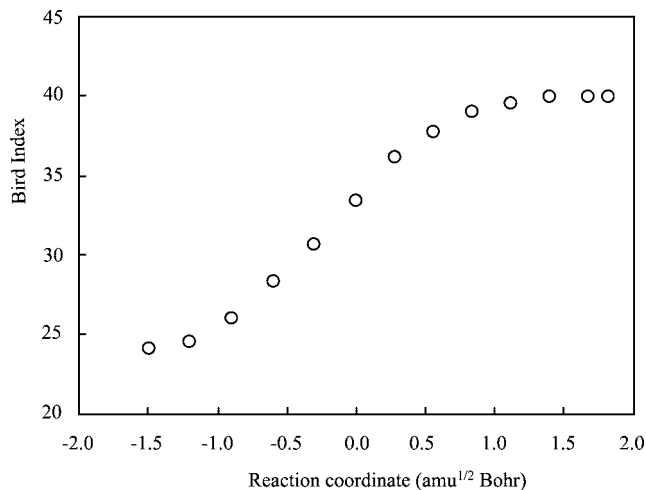to the fact that the respective carbanions derive most of their stabilization from inductive rather than resonance effects which, according to the PNS,[5] must result in a lower intrinsic barrier.

The slope, α, of the line shown in the figure and drawn by excluding the points for $CH_2(CN)_2$ and $CH_3COCHCl_2$ is 0.58 ± 0.04 while the intercept is -4.5 ± 0.6 kcal/mol; if the latter points are included (line not shown), α = 0.61 ± 0.06 and the intercept = -4.8 ± 1.0 kcal/mol. We shall use the former values in our discussion. The α value suggests a transition state that is somewhat more product-like than reactant-like. This is the same qualitative conclusion reached from the β values of 0.31 and 0.35 for the deprotonation of **3H−O** and **3H−S**, respectively, by a series of carbanions; it is the same because in the present case the carbanions play the role of products while in the deprotonation of **3H−O** and **3H−S** they assume the role of reactants.

The intercept of the Brønsted plot, -4.5 ± 0.6 kcal/mol, may again be interpreted as providing an approximate value for the intrinsic barrier ($\Delta H_0^\ddagger$). We note that this $\Delta H_0^\ddagger$ value is lower than the $\Delta H_0^\ddagger$ values for the reactions of **3H−O** (-1.5 kcal/mol, Figure 1) or **3H−S** (-2.1 kcal/mol, Figure 2) with carbanions (eq 7). This is consistent with the notion that the cyanide ion is not a delocalized carbanion and hence the reaction is not subject to the intrinsic barrier enhancing effect of such delocalization.[5]

Regarding the barriers for the reactions of **3H−O**, **3H−S**, **4H−O**, and **4H−S** with CN$^-$ we note that the points for **3H−O** and **3H−S** lie close to the line while the points for **4H−O** and **4H−S** lie above the line. These findings are consistent with the notion that the intrinsic barriers for **3H−O** and **3H−S** are lower than for the corresponding noncyclic analogues **4H−O** and **4H−S**, respectively. The fact that the points for **3H−O** and **3H−S** are close to the line rather than below it is probably the result of barrier enhancing steric crowding at the transition state which counteracts the barrier reducing effect of aromaticity.

Relationship Between Intrinsic Barriers and Aromatic Stabilization. As discussed above, the aromaticity indices provide strong evidence of disproportionately high aromaticity of the transition states of the reactions of **3H−O** and **3H−S** with various carbanions as well as the identity reactions of eq 9. This high transition state aromaticity also manifests itself in the lower intrinsic barrier of the **3H−S/3$^-$−S** identity reaction system compared to that of the **3H−O/3$^-$−O** system, the lower

(26) Feixas, F.; Matito, E.; Poater, J.; Solá, M. *J. Comput. Chem.* **2008**, *29*, 1543.

intrinsic barriers of the identity reactions 9 relative to their respective noncyclic counterparts in eq 10, and of the reactions of **3H−O** and **3H−S** with CN⁻ when compared to the reactions of **4H−O** and **4H−S**, respectively, with the same base. However, the intrinsic barrier lowering effect is much less dramatic than for reactions 1 and 2 (Table 6).

A major reason for the smaller barrier reducing effect may be attributed to the lower aromaticity of **3⁻−O** and **3⁻−S** relative to that of benzene or the cyclopentadienyl anion. For benzene an aromatic stabilization energy (ASE) of −36.3 kcal/mol was calculated based on the isodesmic reaction 12[2] while for cyclopentadienyl anion ASE = −29.4 kcal/mol was obtained based on the isodesmic reaction 13.[2] These ASEs are close to the various literature values obtained by a variety of different methods[2] and
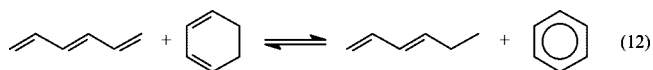
$$\text{(12)}$$
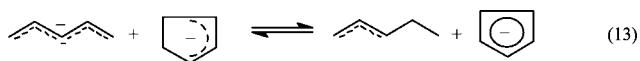
$$\text{(13)}$$

hence were deemed quite reliable.[27] In agreement with the notion that reductions in the intrinsic barriers should be larger when the ASE is larger, the reduction in $\Delta H_0^{\ddagger}$ for the $C_6H_7^+/C_6H_6$ system relative to the [structure]/[structure] system is −11.1 kcal/mol while for the $C_5H_6/C_5H_5^-$ system relative to the [structure]/[structure] system it is −7.6 kcal/mol.

For **3⁻−O** and **3⁻−S** no ASEs have been reported in the literature. Our attempts to calculate such energies based on $\Delta H°$ for the isodesmic reaction 11 yielded ASE = −13.4 kcal/mol for **3⁻−O** and −14.8 kcal/mol for **3⁻−S**. This compares with ASE = −19.8 kcal/mol for furan and −22.4 kcal/mol for thiophene (ΔASE = 2.6 kcal/mol) according to Schleyer et al.,[29] or ASE = −15.0 kcal/mol for furan and −19.5 kcal/mol for thiophene (ΔASE = 4.5 kcal/mol) according to Chestnut et al.[30] Assuming that the isodesmic reactions of eqs 11a and 11b are a reasonable choice for estimating ASEs, one needs to explain why the ASEs are lower than those for the corresponding parent heterocycle and why the difference between the ASEs of **3⁻−O** and **3⁻−S** is so small (ΔASE = 1.4 kcal/mol).

The lower ASEs may reflect the fact that for **3⁻−O** and **3⁻−S** the contribution of the respective resonance structures **a** and **b**, albeit small, may not be completely negligible.

[structures a and b]
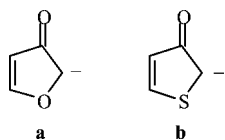
The small difference in the ASEs between **3⁻−O** and **3⁻−S** suggests factors other than aromaticity affect $\Delta H°$ for eqs 11a and 11b. One such factor is the polarizability effect of sulfur[31,32] which is expected to stabilize the four species in eq 11b to different degrees. This is best appreciated when these four species are represented by their alternative resonance structures

as in eq 14. In each structure the polarizability effect of the sulfur stabilizes the negative charge. However, because **3⁻−S**

$$\text{(14)}$$
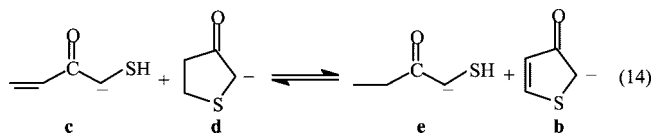
derives much of its stabilization from the aromaticity of its enolate ion resonance structure, the contribution of **b** to the resonance hybrid is much smaller than the contributions of **c**, **d** and **e** to their respective resonance hybrids. As a result, **3⁻−S** benefits less from the stabilizing effect of sulfur than the other three species in eq 11b which tends to stabilize the left side of the equation and make $\Delta H°$ less negative.

A better measure of the *difference* in aromaticity between **3⁻−S** and **3⁻−O** is the 6.7 kcal/mol difference in the acidities of **3H−S** ($\Delta H°_{acid}$ = 349.7 kcal/mol) and **3H−O** ($\Delta H°_{acid}$ = 356.4 kcal/mol). In this comparison the polarizability effect should play a minor role and hence the acidity difference should mainly reflect the difference in the aromaticity of the two anions.

Apart from the lower ASEs for **3⁻−O** and **3⁻−S**, an additional attenuation of the barrier lowering effect of aromaticity comes from charge delocalization. It has been shown that even in reactions involving aromatic systems charge delocalization lags behind proton transfer[2,33] and hence increases the intrinsic barrier. In fact, in systems where the ASE is quite small, the barrier enhancing effect of delayed charge delocalization more than offsets the aromaticity effect and leads to a net *increase* in the intrinsic barrier.[33]

Conclusions

1. The NICS values, HOMA and Bird Indices of the transition states of the reactions of **3H−O** and **3H−S** with various carbanions and of the identity reactions show a high degree of aromaticity, indicating that the development of aromaticity is more advanced than proton transfer. The same conclusion is reached from plots of NICS values and Bird Indices as a function of the reaction coordinate for the reaction of **3H−O** with ⁻CH₂NO₂ and the reaction of **3H−S** with ⁻CH₂NO, showing a sharp increase in these parameters as the transition state is approached.

2. The intrinsic barrier for the identity reactions (eq 9) are lower than for their respective noncyclic reference systems (eq 10), suggesting that the high transition state aromaticity translates into a lower barrier. A similar conclusion is reached from the fact that the barrier for the **3H−S/3⁻−S** system is lower than for the **3H−O/3⁻−O** system, reflecting the higher aromaticity of **3⁻−S** compared to that of **3⁻−O**. The greater aromaticity of **3⁻−S** compared to that of **3⁻−O** also manifests itself in the lower intrinsic barrier of the deprotonation of **3H−S** by CN⁻.

3. The barrier lowering effect of the aromaticity in the reactions of **3H−O** and **3H−S** is substantially smaller than in reactions 1 ($C_6H_7^+/C_6H_6$) and 2 ($C_5H_6/C_5H_5^-$). This mainly reflects the lower ASEs for **3⁻−O** and **3⁻−S** compared to the ASEs for benzene and cyclopentadienyl anion, respectively. There is also an attenuation of the barrier lowering effect of

(27) A referee has pointed out that calculations including hyperconjugation and protobranching corrections suggest an ASE of about 60 kcal/mol for benzene.[28]

(28) Wodrich, M. D.; Wannere, C. S.; Mo, Y.; Jarowski, P. D.; Houk, K. N.; Schleyer, P. v. R. *Chem. Eur. J.* **2007**, *13*, 7731.

(29) Schleyer, P. v. R.; Freeman, P. K.; Jiao, H.; Goldfuss, B. *Angew. Chem.* **1995**, *107*, 332.

(30) Chestnut, D. B.; Gross, P. M. *Chem. Phys.* **2007**, *338*, 75.

(31) Bernasconi, C. F.; Kittredge, K. W. *J. Org. Chem.* **1998**, *63*, 1994.

(32) Anslyn, E. V.; Dougherty, D. A. *Modern Physical Organic Chemistry*; University Science Books: Sausalito, CA, 2006; p 25.

(33) Bernasconi, C. F.; Wenzel, P. J. to be published.

aromaticity by the barrier increasing effect of charge delocalization. This latter effect becomes relatively more important when the aromaticity effect is smaller as is the case when comparing 3^--O or 3^--S with benzene and $C_5H_5^-$.

Calculations

Separated reactants, transition states, and products were calculated at MP2/6−31+G** by using Gaussian 03, Revision C.02.[34] Full frequency analyses were carried out to confirm that the optimized structures were minima or saddle points on the potential energy surface. All activation and reaction energies reported are relative to separated reactants in kcal/mol. We used enthalpies rather than free energies in our discussion, since calculated entropies, and hence free energies as well, are known to be less reliable and not suitable for linear free energy analyses. Aromaticity indices (NICS values, HOMA and Bird indices) were calculated according to the literature (refs 3, 15, and 16) with Gaussian 03.

Supporting Information Available: Table S1 (Structural parameters and energies); Charts S1 and S2 (Transition State Structures); Figures S1−S3 (Plots of r_{C-H}/r_{H-B}, NICS and Bird Index versus IRC); Complete ref 34. This material is available free of charge via the Internet at http://pubs.acs.org.

JO8018076

(34) Frisch, M. J.; et al. Gaussian 03, revision C.02; Gaussian, Inc.: Wallingford, CT, 2004.